



Lanthania promoted MgO: Simultaneous highly efficient catalytic degradation and dehydrochlorination of polypropylene/polyvinyl chloride

Qian Zhou ^{*}, Wenwen Lan, Anke Du, Yuzhong Wang ^{*}, Jiawei Yang,
Yanhui Wu, Keke Yang, Xiuli Wang

Center for Degradable and Flame-Retardant Polymeric Materials, College of Chemistry, Sichuan University, Chengdu 610064, China

Received 17 July 2007; received in revised form 6 November 2007; accepted 22 November 2007

Available online 3 January 2008

Abstract

A lanthania modified MgO catalyst, La-MgO, has been developed and characterized by adsorption methods, X-ray diffraction method (XRD), scanning electron microscopy (SEM), temperature-programmed desorption of ammonia (NH₃-TPD) and CO₂ (CO₂-TPD). The La-MgO has been proved to be a highly efficient and stable dehydrochlorination chemisorbent; moreover, it shows prominent catalytic degradation ability for a typical PVC-containing polyolefins (polypropylene/polyvinyl chloride), i.e., higher degradation rate and superior liquid quality, which will be very useful in the recycling of chlorine-containing waste plastics.

© 2007 Elsevier B.V. All rights reserved.

Keywords: Lanthania promoted MgO; Dechlorination; Catalytic degradation; Polyvinyl chloride; Polypropylene; Recycling

1. Introduction

Recycling of waste plastics is of great interest due to the serious environmental problems caused by waste plastics. Resource recovery from waste plastics, which is regarded as a potential alternative source of energy rather than wastes, is paid much attention nowadays as there will be shortage of the petroleum resource in future. Among the various methods of resource recovery, polymer pyrolysis, aiming to degrade waste plastics to fuel oil or valuable chemicals for a variety of downstream processes, is the most promising technology for resource recovery from waste polymer materials [1]. However, polyvinylchloride (PVC) in waste plastics will cause corrosion problems and a contamination of all product streams with chlorinated organics during pyrolysis. Therefore, the dehydrochlorination of waste plastics is a must for this reaction. Different sorbents for dehydrochlorination were investigated [2,3], and among these sorbents, alkaline earth oxides such as MgO attracted significant attention as effective dehydrochlorination catalysts and chemisorbents. However, they are far from the requirement of realizing commercial use of this process due

to the limited dehydrochlorination degree and fast deactivation of the catalysts caused by large amounts of HCl produced during the reaction. Accordingly, some composite catalysts were developed with high dehydrochlorination stability [4]. On the other hand, lowering degradation temperature and increasing degradation rate, which will decrease energy consumption of this process, are also very necessary for this reaction. Our previous work has developed Al-Zn and Al-Mg composite oxides with both dehydrochlorination and degradation ability [5,6]. However, the stability of the catalysts is unsatisfying. Until now, the development of highly stable and active catalysts with both dehydrochlorination and catalytic degradation ability for this reaction remains a challenging task. In this paper a lanthania modified MgO catalyst, La-MgO, was developed. The catalytic degradation and dehydrochlorination behaviors of La-MgO for polypropylene/polyvinyl chloride (PP/PVC) were investigated.

2. Experimental

2.1. Materials

PP (1300) was obtained from Beijing Yanshan Petrochemical Co., Ltd., China, and PVC (SG-1) from Xian Chemical Co., China. The chlorine content of the PVC was 51.5%.

* Corresponding authors. Tel.: +86 28 85410259; fax: +86 28 85410259.

E-mail address: yzwang@email.scu.edu.cn (Y. Wang).

Magnesium nitrate, lanthanum nitrate and aqueous ammonia were of analytical grade and used as received.

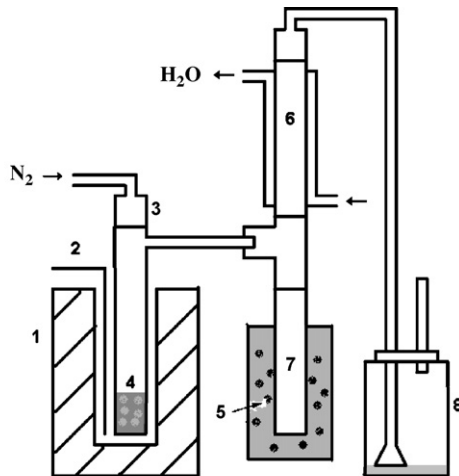
2.2. Preparation and characterization of La-MgO

The La-MgO composite catalyst was prepared as follows: magnesium nitrate and lanthanum nitrate were dissolved in deionized water and precipitated by ammonium hydroxide until the pH value reached 9.5, after the resulting suspension stayed for 1 h at this pH; the precipitate was thoroughly washed with absolute ethanol. The obtained samples were treated under air at 120 °C for 12 h and calcined at 500 °C for 5 h. Without specially noted, the following La-MgO is referred to the one with Mg/La molar ratio of 8.

The powder X-ray diffraction pattern (XRD) was recorded on a Philips X'Pert Pro X-ray instrument with a CuK α X-ray. Surface areas of the composite oxides were calculated using the BET equation from adsorption isotherms of nitrogen measured at liquid nitrogen temperature (AUTOSORP ZXF-4, China). The chemical compositions of the catalyst were determined using ICP (ICP/AES IRIS Advantage, Thermal Elemental, USA) method. Scanning electron microscopy (SEM) analyses were carried out with a JEOL JSM6490LV electron microscope equipped with an EDX analyzer (EDAX Genesis2000). The secondary electron image (SEI) was adopted to characterize catalysts morphology, and backscattered electron image (BES)-elemental analysis was for chemical compositions on the surface of the catalysts. The surface acidity/acid strength distribution of the catalysts were determined by the temperature-programmed desorption of ammonia (NH₃-TPD) on the catalyst (0.1 g) from 100 °C to 600 °C at a heating rate of 10 °C min⁻¹ in a flow of dry helium (30 mL min⁻¹) in a U-shape quartz reactor. The surface basicity/base strength distribution of the catalysts were determined by temperature-programmed desorption of CO₂ (CO₂-TPD) from 50 °C to 600 °C. Before the TPD measurements, the catalyst was pretreated at 600 °C for 1 h.

2.3. Degradation procedure and product analysis

The degradation of PP/PVC was carried out in a glass reactor by batch operation (Fig. 1). Experimental details and product analyses have been described previously [6]. In a typical catalytic run, catalysts (2 g) were mixed with PP/PVC (10 g, in a weight ratio of PP/PVC/sorbents = 4/1/1), and the reactor was heated from room temperature to 120 °C for 60 min under nitrogen flow. Then the N₂ was cut off and the reactor temperature was increased to 330 °C at a heating rate of 10 °C min⁻¹ and held for 20 min. Finally, the temperature was increased to 400 °C and held until no liquid was produced. The products of degradation were classified into three groups, viz., liquid products, which are condensable at 0 °C, gaseous products, and residue. The liquid products were analyzed by gas chromatograph with a flame ionization detector (FID) (FULIYIQI- 9790), and C-NP gram of the liquid products was obtained by plotting the equivalent carbon number of liquid products against the weight fraction of individual components.



1.Furnace; 2.Thermocouple; 3.Reactor; 4.Materials of Pyrolysis; 5.Ice; 6.Condenser; 7.Graduated Cylinder; 8.NaOH trap

Fig. 1. Schematic diagram of the experimental apparatus.

The chlorine in gaseous product was trapped by NaOH aqueous solution and analyzed by chloride ion selective electrode (ISE) method. Moreover, the gaseous HCl dissolved in the liquid phase was also calculated as gaseous chlorine part. The chlorine content of the liquid products, which is calculated according to organic chlorine contents in the liquid products, and chlorine content of residue were analyzed by oxygen bomb combustion and the chlorine ion selective electrode method. The chlorine contents in residue are assumed only from metal chlorides, so by combining with results from XRD measurements, the conversions of lanthania and magnesia to their chlorinated materials were calculated.

3. Results and discussion

3.1. Catalytic degradation of PP/PVC

Fig. 2 illustrates the catalytic performance of the La-MgO catalyst for degradation of PP/PVC. It can be seen that compared with MgO, the La-MgO exhibits a prominently

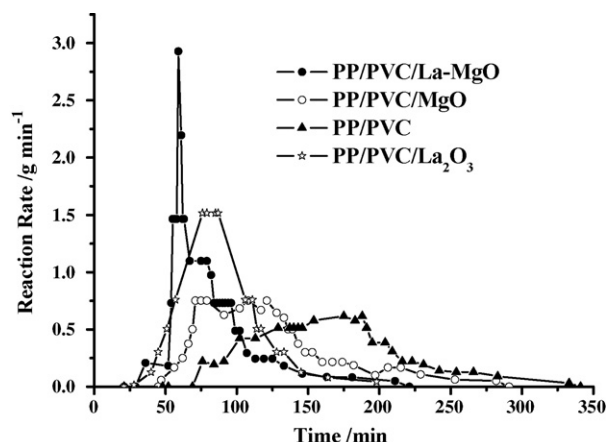


Fig. 2. Liquid production rate for thermal and catalytic degradation of PP/PVC.

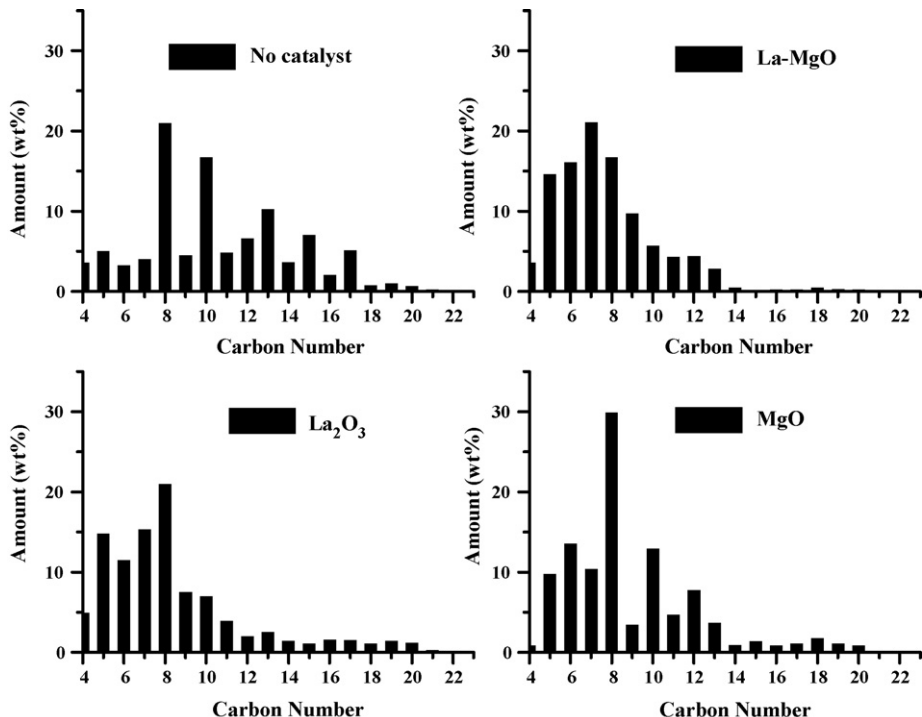


Fig. 3. C-NP gram of liquid products from thermal degradation of PP/PVC.

higher degradation rate so that the reaction can be completed in shorter periods. Moreover, from the carbon number distribution of the liquid products shown in Fig. 3, we can see that the lighter products increase and the heavier decrease, which causes the Cnp (average carbon number of liquid products based on C-NP gram) to sharply decrease from 10.3 (thermal degradation) to 7.6 using La-MgO, proving a deeper degree of degradation. These results confirm prominent catalytic degradation effects of La-MgO for degradation of PP/PVC. Moreover, the La-MgO shows even higher catalytic degradation ability than that of La₂O₃ (Figs. 2 and 3). Generally, the catalytic degradation abilities are directly correlated with the acid properties of catalysts. Fig. 4 shows the acidity and acid intensity distribution

of the catalysts determined by the NH₃-TPD; it can be found that La-MgO shows larger desorption peak area and higher desorption temperature than MgO, suggesting the higher number and intensity of acid sites for La-MgO, which is consistent with the results obtained by Ivanova et al. [7].

3.2. Dehydrochlorination of PP/PVC

For the dehydrochlorination ability of the catalysts (Fig. 5), it can be seen that for thermal degradation of PP/PVC, 78.9 wt.% of chlorine of the original PVC is evolved as gaseous inorganic chlorine of HCl, and as high as 18.5 wt.% of chlorine exists in liquid products. With the addition of MgO to PP/PVC, the

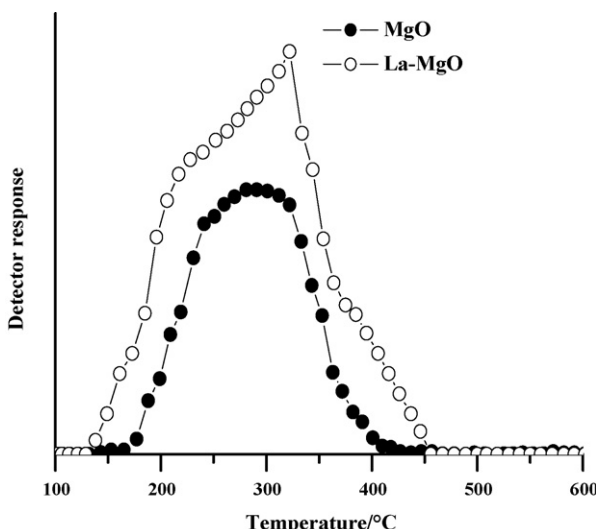
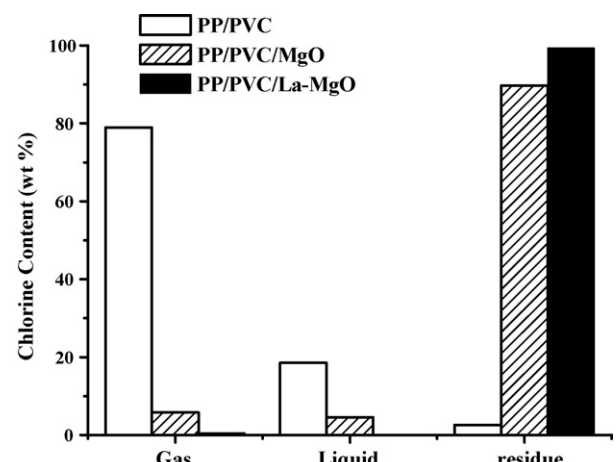
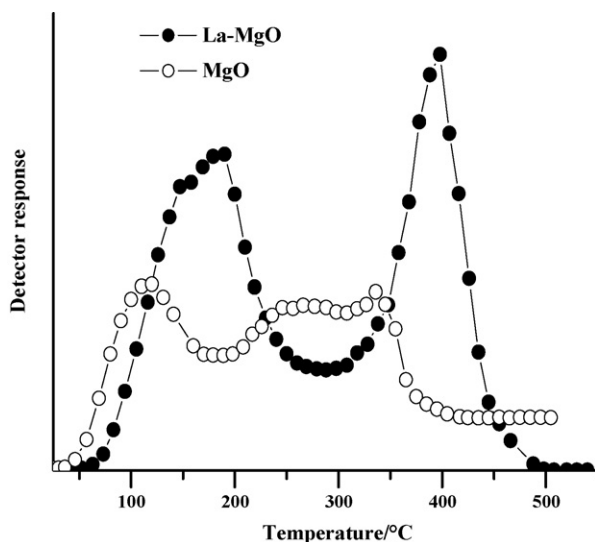
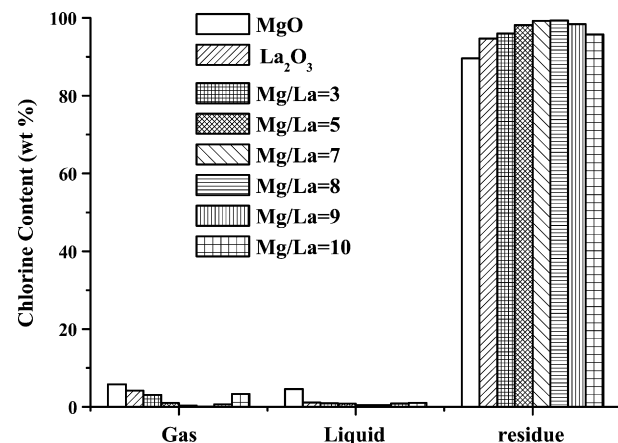
Fig. 4. NH₃-TPD plots of MgO and La-MgO.

Fig. 5. Chlorine distributions from thermal and catalytic degradation of PP/PVC at 400 °C.

Fig. 6. CO_2 -TPD plots of MgO and $\text{La}-\text{MgO}$.

chlorine contents in gaseous and liquid products decrease to 5.8 wt.% and 4.6 wt.%, respectively. Accordingly, about 26.0% of MgO is converted to $\text{MgCl}_2 \cdot 6\text{H}_2\text{O}$, indicating that MgO has certain dehydrochlorination ability. Interestingly, $\text{La}-\text{MgO}$ shows prominently much better dehydrochlorination ability than MgO : the evolved chlorine is sharply decreased to 0.65 wt.%, including 0.54 wt.% as HCl , and 0.11 wt.% in the organic liquid phase.

In fact, $\text{La}-\text{MgO}$ exhibits increased surface area (S_{BET} : $83.5 \text{ m}^2 \text{ g}^{-1}$) relative to MgO (S_{BET} : $55.4 \text{ m}^2 \text{ g}^{-1}$), and the increased interactions between sorbents and the produced HCl during degradation of PP/PVC may contribute the superior dehydrochlorination ability of $\text{La}-\text{MgO}$. Moreover, by comparing the CO_2 -TPD profiles between parent and modified MgO (Fig. 6), it can be seen that the two desorption peaks of $\text{La}-\text{MgO}$, representing weak and strong basic sites, respectively, show increased peak areas and shift to higher temperatures relative to MgO , proving that the number and intensity of both weak and strong basic sites are greatly increased. These results show a strong correlation of the dehydrochlorination ability with the basicity of the catalyst. For $\text{La}-\text{MgO}$, the surface average La/Mg atomic ratio determined by SEM-EDX equals 0.317 that are much higher than the bulk La/Mg ratio of 0.0937 as calculated from the ICP-AES analysis, suggesting the lanthanum enrichment on the $\text{La}-\text{MgO}$ surface. This may

Fig. 7. Effects of magnesium-to-lanthanum molar ratio on the dechlorination ability of $\text{La}-\text{MgO}$.

account for the increased basicity of $\text{La}-\text{MgO}$ due to the higher basicity of lanthanum oxide. From Fig. 7 it can be seen that La_2O_3 does show higher dechlorination ability than that of MgO , i.e., with the addition of La_2O_3 to PP/PVC, the chlorine contents in gaseous and liquid products decrease to 4.2 wt.% and 1.1 wt.%, respectively, and almost all of La_2O_3 is converted to LaOCl and LaCl_3 . On the other hand, under the investigated conditions all the $\text{La}-\text{MgOs}$ with different lanthanum-to-magnesium molar ratio exhibit even higher dechlorination ability than that of La_2O_3 (Fig. 7), and the optimum dechlorination ability is obtained for $\text{La}-\text{MgO}$ with Mg/La molar ratio of 8, suggesting that synergistic effects exist between lanthanum and magnesium oxides. The formation of additional low coordination surface oxygen species by the incorporation of rare earth cations in the MgO lattice that contributes to the increased basicity of $\text{La}-\text{MgO}$ may explain these synergistic effects [8].

The stability of the catalysts was investigated by repeatedly using the same catalysts for up to five consecutive batch processes (Fig. 8). For MgO , with the increase of reaction runs the chlorine contents in both liquid and gas are sharply increased so that for run 5 the evolved chlorine is as high as 68.3 wt.%, indicating that MgO possesses unstable dehydrochlorination ability. Moreover, lanthanum oxide also shows obvious decreased dechlorination ability with the increase of reaction runs. On the contrary, $\text{La}-\text{MgO}$ exhibits much higher stability than MgO and La_2O_3 . After recycling once (Fig. 8, run

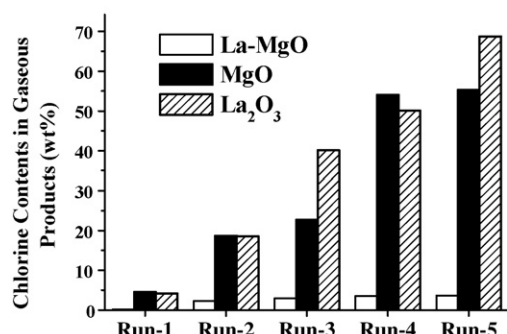


Fig. 8. Effects of catalytic degradation runs on chlorine distribution of PP/PVC.

Table 1

Properties of the fresh and used La-MgO

Catalyst	Atomic ratio ^a		S_{BET} ($\text{m}^2 \text{ g}^{-1}$)	XRD peak
	La/Mg	Cl/O		
MgO-run 1			55.4	MgO
MgO-run 2			18.8	$\text{MgCl}_2 \cdot 6\text{H}_2\text{O}$, MgO
La-MgO-run 1	0.32	–	83.5	Amorphous phase
La-MgO-run 2			21.5	LaOCl
Point A	0.75	0.47		
Point B	0.024	0.16		
La-MgO-run 3			–	LaOCl, MgO
La-MgO-run 4			–	$\text{MgCl}_2 \cdot 6\text{H}_2\text{O}$, MgO, LaOCl
Point A	0.16	0.54		
Point B	0.028	0.21		

^a Obtained by SEM-EDX analysis.

2), the evolved chlorine only slightly increases, i.e., chlorine in gas increases from 0.11 wt.% to 2.23 wt.% and chlorine in liquid from 0.54 wt.% to 2.25 wt.%, and keeps almost constant for the following recycling runs.

According to XRD patterns of the fresh and used MgO, MgO is changed to $\text{MgCl}_2 \cdot 6\text{H}_2\text{O}$ by the reaction of MgO with HCl released from dehydrochlorination of PVC. Moreover, incomplete transformation of MgO to MgCl_2 is observed, suggesting that the produced MgCl_2 crust on the surface of MgO inhibits the reactant to MgO; hence, the dehydrochlorination ability of MgO decreases with the increase of reaction runs. On the other hand, the dramatic decrease of S_{BET} of MgO from $55.4 \text{ m}^2 \text{ g}^{-1}$ to $18.8 \text{ m}^2 \text{ g}^{-1}$ after reaction, which is probably due to pore blocking from MgCl_2 , also leads to the decrease of dehydrochlorination ability of MgO.

From the properties of the fresh and used La-MgO investigated by XRD and SEM-EDX analysis (Table 1, Fig. 9), it can be seen that La-MgO shows an amorphous

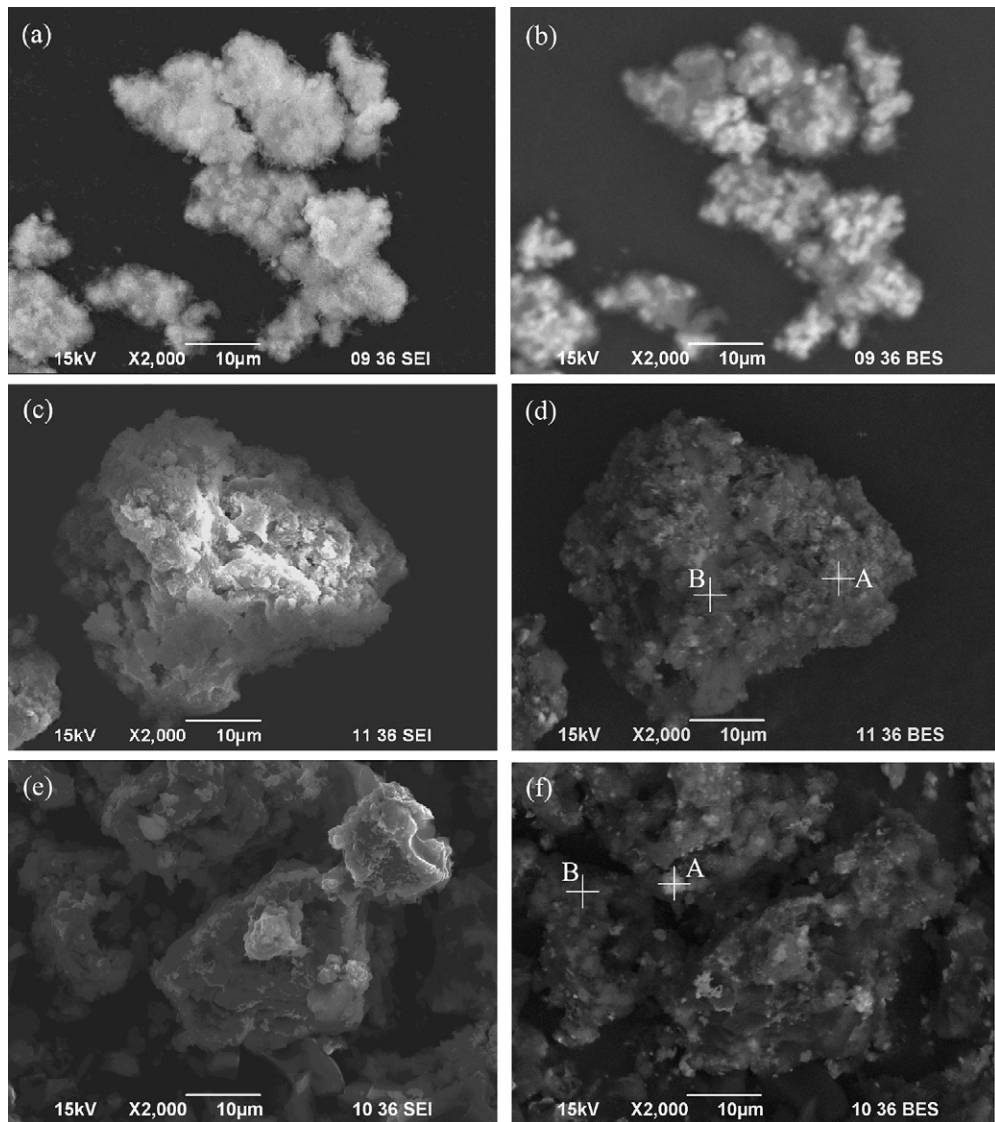


Fig. 9. Scanning electron micrography analysis of the fresh and used La-MgO catalysts (a) La-MgO-run 1/SEI, (b) La-MgO-run 1/BES, (c) La-MgO-run 2/SEI, (d) La-MgO-run 2/BES, (e) La-MgO-run 4/SEI and (f) La-MgO-run 4/BES.

phase with lanthanum and magnesium evenly dispersed on the surface of the catalyst particles (Fig. 9a and b). After reaction (La-MgO-run 2), morphology changes can be observed from SEM-EDX/SEI analysis (Fig. 9c), and lanthanum aggregation is detected from SEM-EDX/BES elemental analysis (Fig. 9d), where point A with white color indicates a lanthanum-rich area ($\text{La/Mg} = 0.75$) and point B with grey color suggests an MgO-rich area ($\text{La/Mg} = 0.024$). Moreover, the chlorine contents are much higher for lanthanum-rich area ($\text{Cl}/\text{O} = 0.47$), indicating higher chlorine fixing degree. From XRD analysis the new XRD peaks assigned to LaOCl are observed, but there is no evidence for crystalline phases of magnesium chloride. On the other hand, SEM-EDX analysis proves that the chlorine element is present on the surface of the catalyst for both lanthanum-rich and magnesium-rich areas. These results suggest that at initial stage dehydrochlorination mainly occurs on lanthanum ion. With the increase of reaction runs (La-MgO-run 4) the chlorine contents for both lanthanum-rich and magnesium-rich area increase. Moreover, a new XRD phase of $\text{MgCl}_2 \cdot 6\text{H}_2\text{O}$ appears, suggesting a deeper dehydrochlorination degree over magnesium ion. The destructive dehydrochlorination process requires the continuous renewing of the metal oxide surface by $\text{O}^{2-}/\text{Cl}^-$ exchange [9–12]. In this case it is believed that lanthanum could enhance the $\text{O}^{2-}/\text{Cl}^-$ exchange rate of La-MgO, therefore, although the S_{BET} of La-MgO decreases from $83.5 \text{ m}^2 \text{ g}^{-1}$ to $21.5 \text{ m}^2 \text{ g}^{-1}$ after reaction, it still keeps the stable dehydrochlorination ability.

4. Conclusions

In summary, the La-MgO proves to be a highly stable and active catalyst with both dehydrochlorination and catalytic degradation ability for PVC-containing plastics (PP/PVC). The addition of lanthanum to MgO results in an increase of both acidity and basicity of MgO, which correlates well with the

prominent higher degradation and dehydrochlorination abilities of La-MgO than those of MgO. Moreover, the enhanced $\text{O}^{2-}/\text{Cl}^-$ exchange rate of La-MgO is responsible for the higher dehydrochlorination stability. The highly efficient and stable catalysts will be very useful in the recycling of chlorine-containing waste plastics.

Acknowledgements

The authors thank the financial support of the National Science Foundation of China (20306019) and the National Science Fund for Distinguished Young Scholars (50525309).

References

- [1] W. Kaminsky, F. Hartmann, *Angew. Chem. Int. Ed.* 39 (2000) 331–332.
- [2] T. Bhaskar, T. Matsui, J. Kaneko, M.A. Uddin, A. Muto, Y. Sakata, *Green Chem.* 4 (2002) 372–375.
- [3] I.V. Mishakov, A.F. Bedilo, R.M. Richards, V.V. Chesnokov, A.M. Volodin, V.I. Zaikovskii, R.A. Buyanov, K.J. Klabunde, *J. Catal.* 206 (2002) 40–48.
- [4] N. Lingaiah, M.A. Uddin, K. Morikawa, A. Muto, K. Murata, Y. Sakata, *Green Chem.* 3 (2001) 74–75.
- [5] C. Tang, Y.Z. Wang, Q. Zhou, L. Zheng, *Polym. Degrad. Stabil.* 81 (2003) 89–94.
- [6] Q. Zhou, C. Tang, Y.Z. Wang, L. Zheng, *Fuel* 83 (2004) 1727–1732.
- [7] A.S. Ivanova, B.L. Moroz, E.M. Moroz, Y.V. Larichev, E.A. Paukshtis, V.I. Bukhtiyarov, *J. Solid State Chem.* 178 (2005) 3265–3274.
- [8] V.R. Choudhary, V.H. Rane, S.T. Chaudhari, *Appl. Catal. A: Gen.* 158 (1997) 121–136.
- [9] K.J. Klabunde, J. Stark, O. Koper, C. Mohs, D.G. Park, S. Decker, Y. Jiang, I. Lagadic, D.J. Zhang, *J. Phys. Chem.* 100 (1996) 12142–12153.
- [10] B.M. Weckhuysen, M.P. Rosyneke, J.H. Lunsford, *Phys. Chem. Chem. Phys.* 1 (1999) 3157–3162.
- [11] S. Decker, I. Lagadic, K.J. Klabunde, J. Moscovici, A. Michalowicz, *Chem. Mater.* 10 (1998) 674–678.
- [12] V.B. Fenelonov, M.S. Mel'gunov, I.V. Mishakov, R.M. Richards, V.V. Chesnokov, A.M. Volodin, K.J. Klabunde, *J. Phys. Chem. B* 105 (2001) 3937–3941.